ORIGINAL PAPER

Effect of Maleated PLA on the Properties of Rotomolded PLA-Agave Fiber Biocomposites

Martín E. González-López[1] · Aida A. Pérez-Fonseca[2] · Erick O. Cisneros-López[2] · Ricardo Manríquez-González[1] · Daniel E. Ramírez-Arreola[3] · Denis Rodrigue[4] · Jorge R. Robledo-Ortíz[1]

Abstract

In this work, agave fibers were surface treated using maleated PLA (MAPLA) in order to increase the fiber content (from 10 up to 40% wt.) in polylactic acid (PLA) biocomposites produced by rotational molding and to study the effect of the agave fiber and its treatment on the physical, mechanical and thermal properties of the biocomposites. This chemical modification between agave fibers and MAPLA was evaluated by FTIR spectroscopy. In general the results indicate that MAPLA surface treatment produces a more homogeneous morphology with lower interfacial gaps and overall porosity, especially at higher agave contents. This improved compatibility promoted better stress transfer leading to increased mechanical properties. For example, the tensile strength and modulus of treated fiber composites increased by up to 68% (from 25 to 41 MPa) and 32% (from 1.30 to 1.74 GPa) respectively, in comparison with untreated fiber composites. Fiber surface treatment also decreases hydrophilicity, lowering water absorption and diffusion coefficient. From thermo–mechanical analyses, the damping behavior of the biocomposites decreased with MAPLA treatment since a stronger interface is able to sustain higher stresses and dissipates less energy. Finally, the thermal stability was also improved as a result of better interfacial chemical bonding leading to a 12 °C increase in thermal stability (from 254 to 266 °C).

Keywords Surface treatment · Biocomposite · Biopolymer · Rotomolding · Agave fibers · MAPLA

Introduction

Recently, environmental problems related to petroleum-based polymers and concerns about carbon footprints are driving an increased development of biodegradable and sustainable biopolymers such as polylactic acid (PLA), polybutylene succinate (PBS) or adipate (PBA), and poly-hydroxyalkanoates (PHA) [1]. Among all the biopolymers available today, PLA has received special interest as it can be produced by ring-opening polymerization of lactide: the cyclic dimer of lactic acid, obtained from renewable sources [2]. So far, PLA has been used for packaging, automotive and medical applications due to its high mechanical strength, easy processability and biodegradability [3–5]. Despite of these advantages, PLA has some drawbacks such as brittleness, mechanical and thermal instability at high temperature (due to its softening around 60 °C), and relatively high cost [6]. Nevertheless, some of these disadvantages may be overcome by different strategies such as plasticization [7], blending with other biopolymers [8, 9] and the production of composites and green biocomposites by the addition of natural fibers [6].

Reinforcing petroleum- or bio-based polymers with lignocellulosic fibers has been a matter of increased interest because of high specific properties, low cost, low density, worldwide availability and biodegradability, as well as their eco-friendly and renewable nature [10, 11]. Natural fibers represent a good reinforcing material for PLA based biocomposites since they keep the biodegradable aspect of the whole biocomposites [4]. However, numerous hydroxyl

✉ Jorge R. Robledo-Ortíz
  jorge.robledo@cucei.udg.mx

1 Departamento de Madera, Celulosa y Papel, CUCEI, Universidad de Guadalajara, Carretera Guadalajara-Nogales km 15.5, Las Agujas, Zapopan, Jalisco 45510, Mexico

2 Departamento de Ingeniería Química, CUCEI, Universidad de Guadalajara, Guadalajara, Jalisco, Mexico

3 Departamento de Ingenierías, CUCSUR, Universidad de Guadalajara, Autlán de Navarro, Jalisco, Mexico

4 Department of Chemical Engineering and CERMA, Université Laval, Quebec City, QC, Canada

groups are present on the surface of natural fiber bundles leading to poor compatibility with most polymer matrices [12]. In composites, the stress must be transferred from the matrix to the reinforcement through the interface. So efficient stress transfer depends on the adhesion level between the components [13]. Therefore, interfacial adhesion must be improved via thermal, physical or chemical fiber surface modifications, as well as the use of coupling agents.

Coupling agents are molecules with functional groups, which can react with the hydroxyl groups on the fibers' surface and entangle with the matrix to improve interfacial adhesion and stress transfer. Over the years, different chemical compounds, such as silanes have been used as coupling agents [14–16]. For example, Orue et al. [17] modified sisal fibers with an alkali–silane treatment to improve the mechanical properties of injection molded PLA biocomposites. The tensile strength was increased by up to 15% at 40% fiber content, while the composites using untreated fibers presented decreases by up to 43%.

According to the literature, maleated polymers have shown significantly improvement on the fiber–matrix compatibility [18, 19]. For PLA, several authors have incorporated maleated PLA (MAPLA) through extrusion compounding and reported that only a certain amount of grafted polymer is required to saturate the interface and achieve good compatibility. For example, Gunning et al. [20] reported increases in tensile and flexural strength of injection molded PLA/jute and PLA/hemp composites with MAPLA. Nevertheless, these properties decreased above an optimum amount (10% wt.) suggesting that an excess of MAPLA (which does not interact at the interface) disrupts the biocomposite matrix (acting as a plasticizer). Yu et al. [21] reported similar trends for compression molded short ramie fiber/PLA biocomposites. In this case, increasing the MAPLA content above 3% wt. decreased the tensile and flexural strength. It is expected that the lower molecular weight of MAPLA due to the functionalization reaction decreases the mechanical properties of compatibilized biocomposites [22]. Another strategy to improve compatibility is the incorporation of reactive molecules during extrusion compounding (reactive extrusion also called one-step compatibilization). Nevertheless, reactive compatibilization may also degrade the matrix if the concentration of maleic anhydride (MA) and dicumyl peroxide are set over the optimum value [23]. Lv et al. [24] reported tensile strength increases by up to 144%, but also suggested that above the optimum MA content (1% wt.) the excess stays at the interface increasing the distance between the chains and decreasing the mechanical properties of the resulting biocomposite.

One way to overcome these mentioned drawbacks is to limit the presence of the coupling agent only at the interface by coating the fibers; i.e. direct surface treatment. Besides, the low-shear conditions related to rotational molding make difficult the direct incorporation of coupling agents without a preliminary compounding step as in extrusion or injection molding. In this sense, Jiang et al. [25] grafted PLA on the hydroxyl groups of sisal fibers by ring-opening polymerization using tin based catalysts. They obtained increases in tensile strength (101%) and modulus (132%) of compression-molded biocomposites showing that graft polymerization can improve interfacial compatibility. In general, strategies to increase interfacial adhesion in composites have shown that chemical interlocking occurs at the interface via esterification reactions, but also van der Waals interactions or hydrogen bonding are expected [12].

Although a large amount of information about PLA-natural fiber biocomposites can be found in the literature, especially for compression and injection molding, there is very limited information on these materials being produced by rotational molding. Greco and Maffezzoli [26] first reported on the production of a rotomolded biocomposite based on plasticized PLA reinforced with the wooden backbone of nopal cactus. They reported flexural properties increase (stiffness, strength and toughness) for composites reinforced with 2.3% wt. of wooden backbone.

According to our knowledge, this work is one of the first reports about the direct coating of natural fibers with MAPLA. Therefore, the objective of this study is to carry out the surface treatment of agave fibers with MAPLA in order to improve compatibility and to evaluate whether fiber content could be increased in rotomolded PLA-agave fiber biocomposites while maintaining acceptable mechanical properties. Thus, the effect of MAPLA grafting onto agave fibers is reported with results on physical, mechanical and thermal properties of rotomolded biocomposites.

Experimental

Materials

Two types of polymers were used. The PLA used for MAPLA preparation was an extrusion grade PLA Ingeo 7001-D from Nature Works (USA) with a melt flow rate (MFR) of 6 g/10 min (210 °C, 2.16 kg) and a density of 1.24 g/cm^3. For the rotomolded composites, the matrix was PLA Ingeo 3251-D from Nature Works (USA) with a MFR of 80 g/10 min (210 °C, 2.16 kg) and a density of 1.24 g/cm^3. PLA 3251-D was first ground into powder using an ultra-centrifuge mill Retsch model ZM 200 operating at 18,000 rpm to obtain the particle size distribution (average size of 40 μm) needed for rotomolding. Agave fibers (*A. tequilana* Weber var. Azul) with particles size between 297 and 400 microns were used as reinforcement. For the functionalization reaction, MA and dicumyl peroxide (Sigma-Aldrich, USA) were used. Finally, *N,N*-dimethylformamide

(DMF, J.T. Baker), acetone, chloroform and methanol (Golden Bell, Mexico) were used as solvents and for characterization.

Polylactic Acid Functionalization

PLA was functionalized through reactive extrusion via free-radical grafting using a Thermo Scientific Process 11 twin-screw extruder. After preliminary trials, the temperature profile was set to 165–170–180–165 °C, while the screw speed was 30 rpm. The proportions of the materials were 100:5:0.2 wt. of PLA, MA and dicumyl peroxide (initiator). MA and dicumyl peroxide were first dissolved in acetone (2 mL acetone/g MA) and added to the polymer. Then, the acetone was evaporated and the impregnated granules were dried overnight in an oven at 60 °C prior to extrusion. MAPLA strands of 1.2 mm in diameter were obtained and pelletized for further use. In terms of characterization, grafting degree was determined by a viscometric titration method according to Lu et al. [27]. For purification, the pellets were dried for 24 h in an oven at 60 °C allowing the unreacted anhydride to evaporate. Then, 1.15 ± 0.05 g were dissolved in a 3:2 (v/v) solution of chloroform and methanol and the solution was titrated against 0.01 N KOH using phenolphthalein as indicator. An average value of 1.9% wt. of grafted MA on PLA was obtained.

Fiber Surface Treatment

The surface treatment was applied to agave fibers by using a 3% wt. MAPLA solution in DMF. The fibers were previously dried in an oven at 60 °C for 24 h and placed in the solution with a fiber/solution ratio of 1:10 under intense stirring at 95 °C for 90 min. After the treatment, the solvent was separated from the fibers by decantation and the recovered fibers were sundried to evaporate the remaining solvent and then placed in an oven at 60 °C for 24 h prior to material compounding.

Biocomposites Preparation

To study the effect of surface coupling on interfacial adhesion, untreated fiber biocomposites (UFBC) and treated fiber biocomposites (TFBC) were prepared with different fiber contents (0–40% wt.). Both treated and untreated fibers were dried overnight in an oven at 60 °C prior to compounding and a dry-blending technique was used to disperse the fibers in the biopolymer matrix using a kitchen blender operating at 3750 rpm during 4 min. Then, the dry-blends were rotomolded in a laboratory-scale rotational molding machine with a rectangular-shaped stainless steel mold of 15 cm × 15 cm × 16 cm and 2 mm in wall thickness. Roto-molding process was performed as follows: (1) preheating

the oven at 300 °C, (2) loading 350 g (corresponding to a final average wall thickness (ε) between 1.9 and 3.6 mm depending on fiber content) of the dry-blended mixture in the mold and heating inside the oven for 24 min with a rotational ratio of 4:1 [19], (3) cooling with air convection for 24 min, and (4) demolding. From the rotomolded parts, different geometries were cut for characterization using a laser-cutting machine (Guian model GN-600LS) at 5 mm/s with a laser intensity of 25 mA.

Fourier Transform Infrared Spectroscopy (FTIR)

Changes in functional groups between the treated and untreated agave fibers were evaluated by collecting FTIR spectra on a Spectrum 100 Fourier transform infrared spectrometer (Perkin Elmer, USA) with ATR accessories. The spectra were obtained from 50 scans at a resolution of 4 cm^{-1} from 4000 to 700 cm^{-1}.

Morphology

Micrographs of the treated and untreated fibers, as well as the exposed surface of impact fractured composite samples, were taken on a scanning electron microscope (SEM) TES-CAN MIRA 3 LMU at different magnifications to observe fiber modification and to characterize the state of fiber adhesion/dispersion in the matrix.

Density and Porosity

The skeletal density and the bulk density of the UFBC and TFBC, as well as neat PLA and the biocomposites, were determined. The skeletal density (ρ_s) was measured by a gas pycnometer ULTRAPYC 1200e (Quantachrome Instruments, USA) using nitrogen. The real density of the treated and untreated agave fibers was also determined. The bulk density (ρ_b) was determined according to ASTM D2395. It was possible to estimate the treated and untreated biocomposites porosity from the differences in the skeletal and bulk density as [28, 29]:

$$Porosity\,(\%) = \left(1 - \frac{\rho_b}{\rho_s}\right) \times 100 \tag{1}$$

Mechanical Properties

Tensile and flexural properties were measured on a universal testing machine (Instron Ceast 3345) equipped with a 1 kN load cell. For tensile testing, type V samples were cut in the parts and the crosshead speed was set at 5 mm/min according to ASTM D638. For flexural testing, the crosshead speed was set at 2 mm/min according to ASTM D790. In both cases, the reported values of strength and modulus

represent the average of at least five samples. Charpy impact strength was determined using an Instron Ceast model 9050 impact tester according to ASTM D6110. The samples were notched with a manual notcher Instron Ceast 6897 and the reported values are the average of a minimum of eight samples. Finally, hardness was measured with a Titanium 0–90HD durometer according to the Shore D scale (thermoplastics) and the values reported are the average of at least 10 measurements.

Water Absorption

The effect of surface treatment on water absorption was determined according to ASTM D570. For this purpose, 2.54×2.54 cm^2 (1×1 in^2) samples were initially dried to constant weight to determine their initial weight (w_i). Then, the samples were immersed in water and placed in an oven at 50 °C. Each sample was smoothly dried before measuring its weight (w_f) at different time intervals. Furthermore, water absorption data was fitted to a Langmuir diffusion model to determine the diffusion coefficients [30]. This model has been used to analyze the water absorption behavior of composites, which often deviates from the Fickian model. The Langmuir diffusion model, proposed by Carter and Kibler [31], introduces two parameters, β and α, to describe the probability of free moisture molecules to become bound or bound molecules to become free, respectively. The equation for 1-D diffusion can be written as:

$$\frac{M_t}{M_\infty} = 1 - \frac{\beta}{(\beta + \alpha)}e^{-\alpha t} - \frac{\alpha}{(\beta + \alpha)}\frac{8}{\pi^2}e^{\frac{-D\pi^2 t}{l^2}} \quad (2)$$

where M_t represents the water absorption at any time, M_∞ represents the water absorption at equilibrium and D is the diffusion coefficient.

Thermal Properties and Dynamic Mechanical Thermal Analyses

Thermal stability of the biocomposites was studied by thermogravimetric analyses. This was performed on a TA Instruments (USA) model Q5000IR. Between 6 and 10 mg of the material was heated from 50 to 800 °C at a constant rate of 10 °C/min under a nitrogen atmosphere (20 mL/min). The biocomposites were also characterized by a dynamic mechanical analyzer (DMA) RSA 3 (TA Instruments, USA) using rectangular specimens with approximate dimensions of $40 \times 12.4 \times \varepsilon$ mm^3. The tests were performed in the linear deformation region (0.02% strain) using a three-point bending geometry ($16 \times \varepsilon$ mm span). The analysis was carried out increasing the temperature from 40 to 100 °C at a rate of 2 °C/min using a frequency of 1 Hz.

Results and Discussion

Fourier Transform Infrared Spectroscopy

Figure 1 shows the FTIR spectra of the agave fibers and agave fibers-g-MAPLA. In the case of untreated agave fiber, the spectrum clearly shows the characteristic absorption bands pattern for lignocellulosic fibers. A broad absorption band around 3330 cm^{-1} is attributed to the hydroxyl (–OH) groups, a peak at 2890 cm^{-1} is characteristic of aliphatic C–H bonds in carbohydrates (cellulose and hemicelluloses), the carbonyl stretching signal of aldehyde group is present at 1740 cm^{-1} attributed to pectins, waxes and lignins, and finally peaks at 1640 and 1510 cm^{-1} (double bonds and aromatic rings) indicating the presence of lignins. Polysaccharide compounds are also confirmed by C–O bonds signal at 1020 cm^{-1} (cellulose and lignins) [16, 18, 25]. The main difference with the treated fibers is the increased intensity of the carbonyl stretching signal, indicating the presence of PLA on the fibers' surface. Jiang et al. [28] found a band at 1772 cm^{-1} due to an ester carbonyl after the ring-opening polymerization of lactic acid. In our case, the PLA carbonyl ester band overlapped with the aldehyde band from agave fibers. Moreover, the new ester bond between agave fibers and MAPLA also contributes to increase the intensity of the signal. The presence of MAPLA on the surface can also be inferred from a small peak in the aliphatic C–H zone at 2995 cm^{-1} corresponding to methyl groups present in the PLA structure which is confirmed with the signals at 1460 and 1380 cm^{-1} (CH$_2$ and CH$_3$). On other hand, a new signal is observed at 1660 cm^{-1} and can be attributed to C=O stretching vibration of the carboxylate group from MA (which is not bonded to agave fibers) as well as the C–O signals at 1190 and 1090 cm^{-1} (different from the
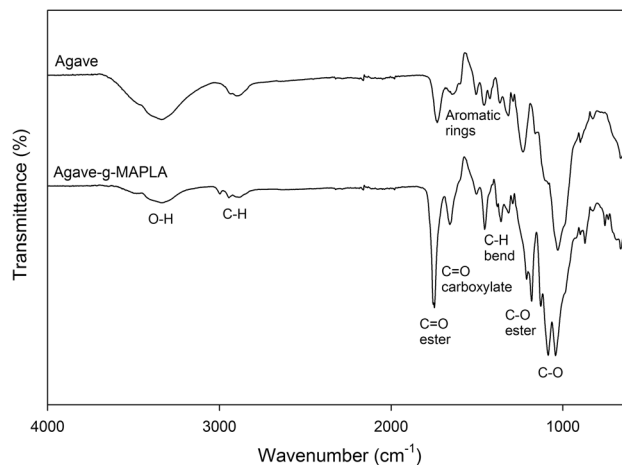

Fig. 1 FTIR spectra of untreated and treated agave fibers with MAPLA

lignocellulosic compounds band at 1020 cm^{-1}) indicate the presence of PLA and suggest that a esterification reaction took place [32]. The intensity decreases of the hydroxyl band at 3330 cm^{-1} also suggests that hydroxyl groups have reacted [33].

Morphology

The morphology of the fibers is presented in Fig. 2. In contrast with the rough surface of the untreated fibers, the surface of treated fibers with MAPLA is smooth and pores are observable due to the removal of non-cellulosic materials from the surface during treatment. It is usually reported that the removal of waxes, hemicelluloses and lignins occurs with alkali treatments (mercerization) [34, 35], suggesting that besides the MAPLA treatment itself, DMF also extracts some of these components. However, the presence of a biopolymer layer on the surface is clearly visible. It is also expected that this polymer layer could have penetrated the fiber's porosity forming a mechanical anchored layer on the surface as well as being chemically grafted through MA, enhancing its compatibility/adhesion with the PLA in both cases [36]. In terms of chemical bonding, the anhydride groups grafted on the PLA backbone promote the esterification reaction with the hydroxyl groups of cellulosic fibers, allowing the formation of a strong interface due to covalent or hydrogen bonding [24].

For the biocomposites, SEM micrographs at 20% agave fibers are shown in Fig. 3. In general, the fractured surface of UFBC presents pull-out and debonded fibers (Fig. 3a) indicating that interfacial bonding is weak [16]. Also, poor dispersion is clearly visible since no fiber can be seen in several

parts of the biocomposite structure. However, the presence of fractured fibers is more evident in TFBC (Fig. 3b) indicating that good compatibility is achieved and the stress was successfully transferred to the fibers. Csikós et al. [37] stated that the incorporation of MAPLA through extrusion led to fiber fracture being the dominating failure process. This can be explained by the presence of the polymer layer on the fiber's surface decreasing its hydrophilicity and improving interfacial adhesion [25]. At higher magnification, it is clear that interfacial gaps observed in UFBC (Fig. 3c) are no longer present with better compatibility associated to the MAPLA treatment (Fig. 3d). Furthermore, above 20% agave, there is high surface area to cover and there is not enough polymer to fill all the volume between the fibers. As shown in Fig. 3e, f, at 30% agave, several gaps are observed since the polymer could not penetrate through the spaces between the fibers, leading to poor mechanical properties as discussed in the following sections. However, much better fiber wetting is observed when treated fibers are used. This also explains why 40% UFBC could not be processed, while 40% TFBC was possible despite having low mechanical properties as discussed in the following sections.

Density and Porosity

The density and porosity of the pure PLA and the biocomposites are shown in Fig. 4. The fiber density was found to decrease by the presence of polymer since a lower density material (PLA density is lower than agave fiber) is added. This observation is consistent with the literature since similar behaviors have been reported for maleated polyethylene surface treated fibers [18, 38].
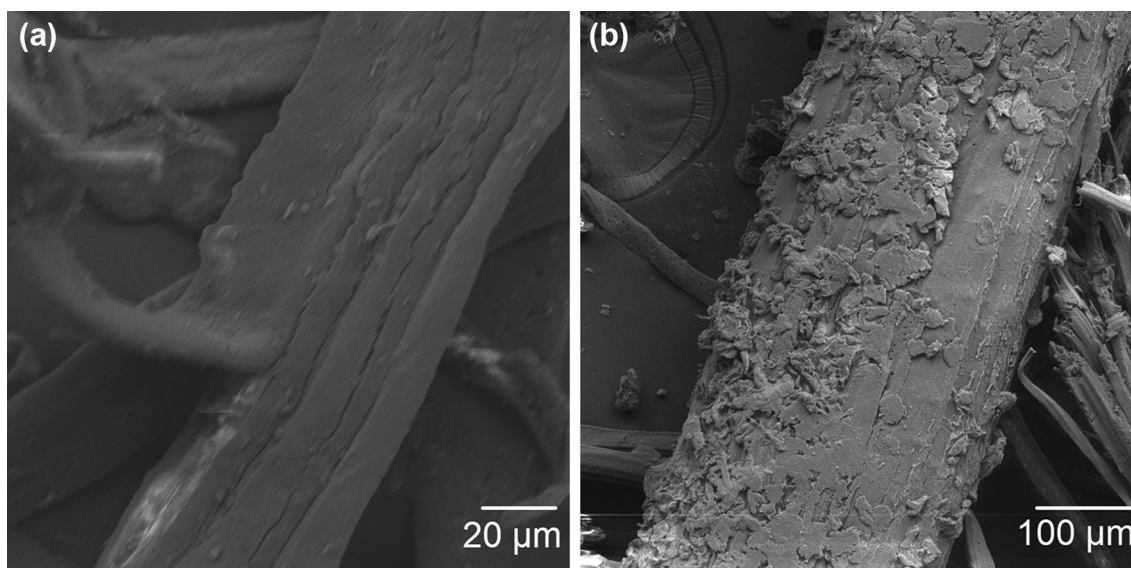

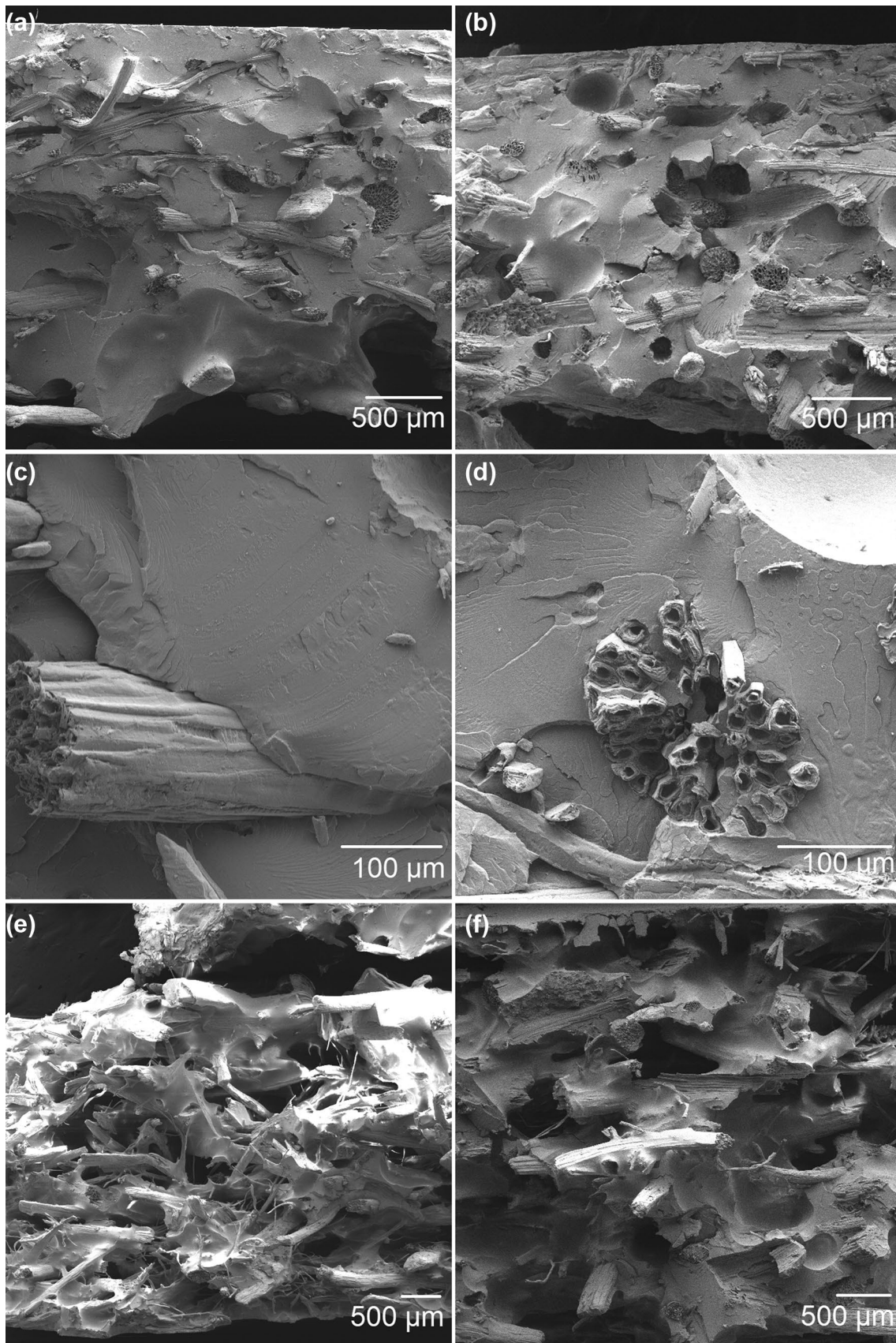**Fig. 2** Typical micrographs of: (**a**) untreated and (**b**) treated agave fibers

Fig. 3 Typical micrographs of UFBC (**a, c**) and TFBC (**b, d**) at 20% wt. agave fiber, as well UFBC (**e**) and TFBC (**f**) at 30% wt. agave fiber
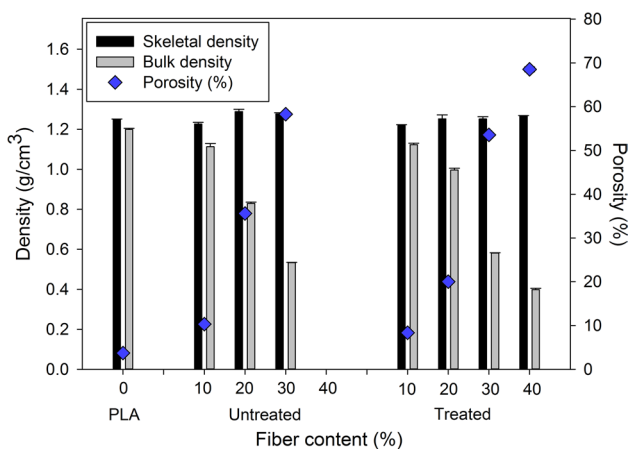
Fig. 4 Density and porosity of UFBC and TFBC

Hardness and Impact Strength

Figure 5a presents the hardness values of PLA, UFBC and TFBC. Shore D hardness measures the resistance of the material to penetration, which tends to decrease with the flexibility and mobility of the polymer chains [40]. In this sense, Teymoorzadeh and Rodrigue [41] reported that Shore D hardness increases for PLA/wood flour composites as a consequence of increased stiffness due to wood addition which decreases the polymer chains mobility and thus the flexibility of the biocomposites. However, hardness is expected to decrease with fiber content in rotomolded composites since no pressure is applied while molding and no compaction is achieved during this low-shear processing [18]. This trend was observed for UFBC since the addition of higher fiber contents decreased the hardness, probably resulting from interfacial gaps due to incompatibility. It is observed in Fig. 5a that the addition of 10% of agave fiber decreases the PLA hardness from 81 to 70 Shore D and decreases even more with increasing fiber content. On the other hand, fiber treatment led to increased hardness in comparison with UFBC. It is noticeable that hardness remains practically unchanged even at 30% agave (68 Shore D) indicating that interfacial gaps presence was decreased because of fiber treatment (Fig. 5a). It has been reported that hardness can also increase as a result of chemical bonding at the interface promoted by MA [42]. Very similar results were obtained by Cisneros-López et al. [19] for linear medium density polyethylene (LMDPE) composites reinforced with agave fibers treated with MAPE, suggesting that increases could be associated with enhanced compatibility leading to lower voids.

Figure 5b reports the results for impact strength. In this case, decreasing values are also observed due to agave fiber
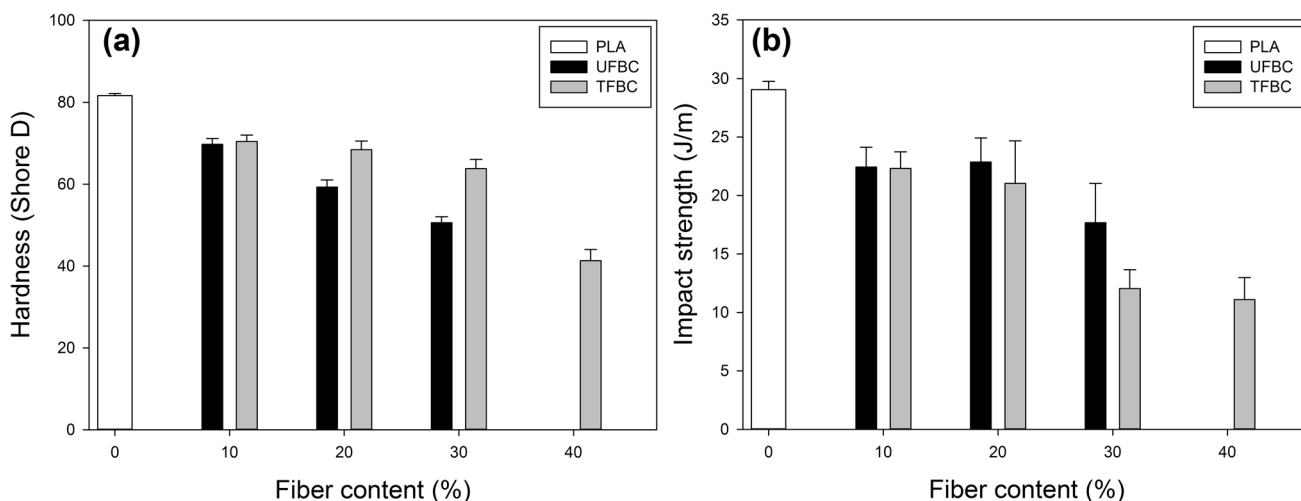
For the biocomposites, the density of UFBC increases with agave fiber, reaching a maximum at 20% fiber content and then decreases. This behavior represents a balance between adding higher density materials (fibers) and more voids being created due interfacial incompatibility increasing the porosity; i.e. more voids and gaps are present as seen in Fig. 3 [39]. For TFBC, despite having lower density than UFBC because of the lower density of treated fibers as discussed above, the density increases with fiber content even up to 40%. This indicates that the MAPLA surface treatment was successful in promoting interfacial compatility between the phases and reducing the voids (overall porosity) in the biocomposites as was observed in Fig. 3. This substantial difference between the morphology of treated and untreated fibers will have an effect on the macroscopic behavior of the biocomposites as described next.

Fig. 5 Shore D hardness (**a**) and impact strength (**b**) of UFBC and TFBC

addition (24% lower in comparison to neat PLA). It was observed that using fiber contents of 10–20% led to similar impact strengths (22 J/m) for UFBC and TFBC, while lower impact strengths are observed at higher fiber contents. The presence of fibers promotes the concentration of stress inducing fracture [25]. However, the impact strengths are lower for TFBC than UFBC since good compatibility promotes good stress transfer and the fibers are fractured with the matrix, while in UFBC the fibers are detached from the matrix (pull-out) during the fracture due to poor adhesion allowing higher energy dissipation and consequently higher values of impact strength [43]. It is known that fibers pull-out increases the distance by which the fracture is propagated, resulting in higher energy absorption by the composite [44].

Tensile Properties

The results for tensile strength and modulus are presented in Fig. 6. It can be seen that the tensile strength of PLA was reduced from 61 to 40 MPa at 10% of untreated agave fiber and lower values are obtained with higher fiber contents. This behavior is associated to interfacial incompatibility, high porosity and fiber agglomeration. A similar trend was observed by Jiang et al. [25] who related the decreasing trend to poor interfacial compatibility between sisal fibers and PLA in compression molded composites. Furthermore, Jandas et al. [36] reported decreasing tensile strength after the incorporation of 30% wt. banana fibers in PLA biocomposites produced by compression molding as a result of poor stress transfer across the interface due to agglomeration. Rotomolded composites are more sensitive to fiber agglomeration because of its low shear/pressure characteristics [18]. Despite showing the same behavior,

TFBC has much higher tensile properties than UFBC. For example, 11% higher of strength (from 40 to 44 MPa) and modulus (from 1.89 to 2.04 GPa) at 10% of fiber content. It is important to notice that tensile properties did not decrease to the same extent as in UFBC. In fact, at 20% wt. of agave fiber, the tensile strength was improved by 68% (from 25 to 41 MPa), while the modulus increased 32% (from 1.30 to 1.74 GPa) in comparison with UFBC. These results indicate that compatibility was improved and better stress transfer was achieved. Nevertheless, in both cases, the tensile properties substantially decreased and no difference was observed at 30% agave. This behavior can be explained because at high fiber contents, PLA could not penetrate between the fibers during rotational molding and several gaps occurred in the biocomposite as observed by SEM (Fig. 3) and this phenomenon dominates over interfacial incompatibility.

Flexural Properties

Figure 7 reports on the flexural properties of PLA and the biocomposites. Flexural strength and modulus present important decreases when agave fiber is added to the PLA. In terms of TFBC at 10% agave, the flexural strength increased from 50 to 55 MPa and the modulus from 2.4 to 3.0 GPa in comparison with UFBC. Furthermore, the TFBC with 20% of fiber content also presented a slight increase in comparison with UFBC. This behavior can be explained by the improved dispersion and lower level of fiber agglomeration induced by the surface treatment. As in the properties presented before, it is also observed that fiber contents higher than 20% produced important decreases in the flexural properties as for tensile ones (Fig. 6).
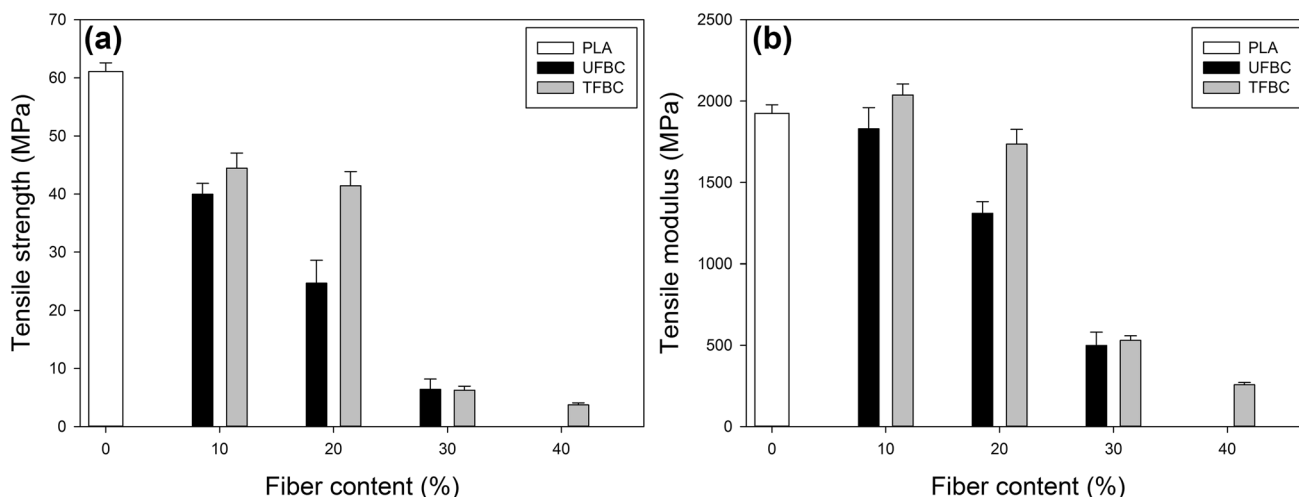

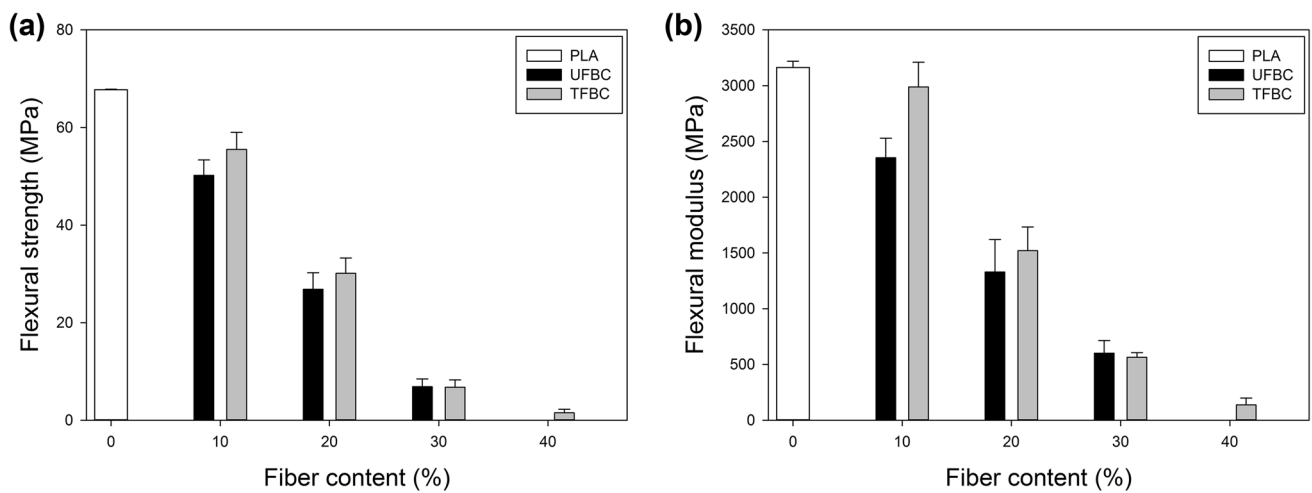Fig. 6 Tensile strength (**a**) and modulus (**b**) of UFBC and TFBC

Fig. 7 Flexural strength (**a**) and modulus (**b**) of UFBC and TFBC

Dynamic Mechanical Thermal Analysis (DMTA)

The results for dynamic ramp test are shown in Fig. 8. In all cases, the elastic modulus (storage modulus) E′ decreases as a function of fiber content as reported for tensile (Fig. 6) and flexural (Fig. 7) moduli. It is also noticeable that E′ sharply decreases between 50 and 60 °C which corresponds to the glass transition temperature of PLA [16]. At this point, the
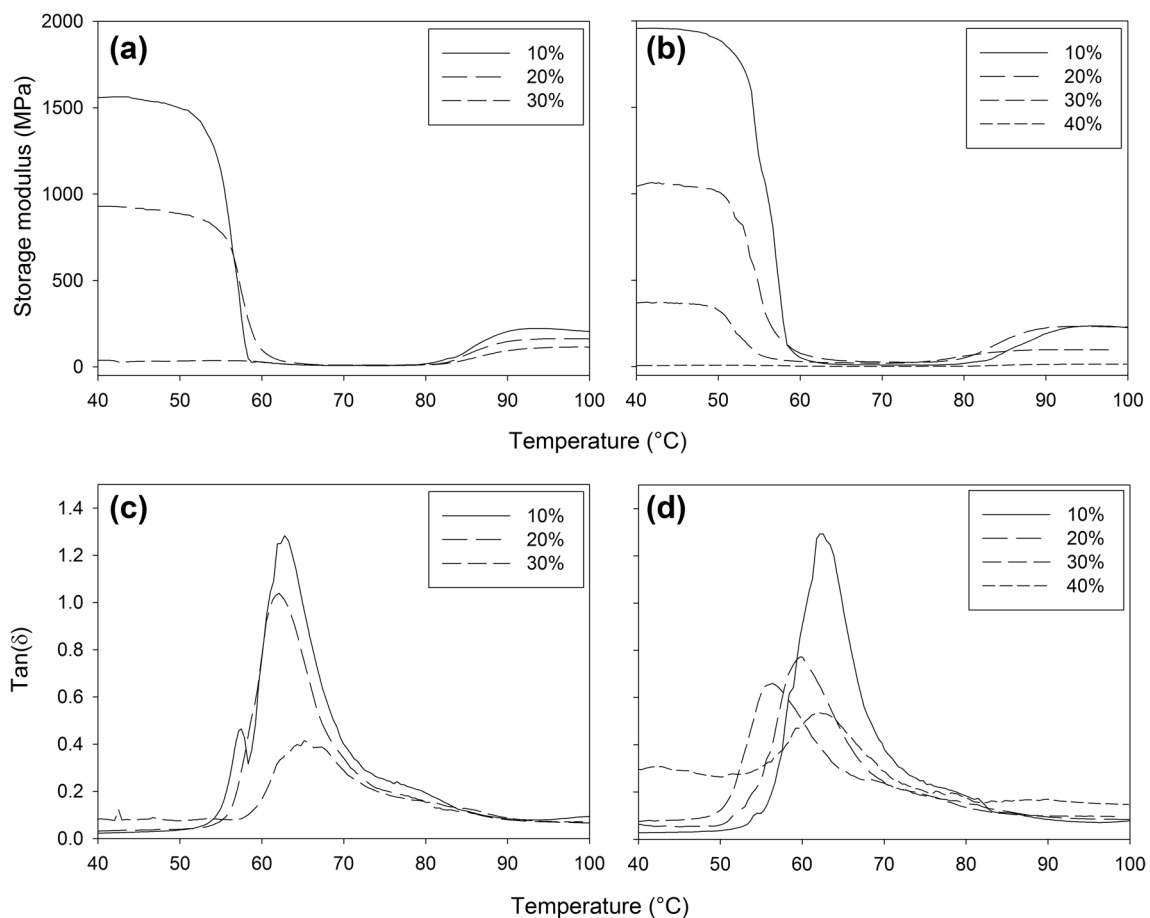

Fig. 8 Storage modulus (E′) and tan(δ) of UFBC (**a**, **c**) and TFBC (**b**, **d**) at different agave contents

material softens and losses stiffness. However, E′ increases between 80 and 90 °C due to the cold crystallization behavior of PLA taking place during the test thus increases the strength of the composite [22, 26, 41]. At all fiber contents, E′ is higher when the surface treatment was applied. Below T_g (between 35 and 55 °C), for composites with 10% agave, the storage modulus is 1.49 GPa (UAF) and 1.88 GPa (TAF), while at 20% agave the values are 0.88 GPa (UAF) and 1.01 GPa (TAF). But higher differences are observed at 30% agave with 35 MPa (UAF) and 71 MPa (TAF), indicating that for treated fibers, better stress is transferred from the matrix to the fibers which increases the biocomposite stiffness. Yu et al. [15] reported higher storage modulus values for ramie fiber composites as a result of alkali and silane treatments, attributing this to better interfacial adhesion. Besides, the E′ values also increased after cold crystallization due the treatment. In this case, interfacial crystallization could increase stress transfer improving the properties of the composite [45]. This suggests that improved compatibility achieved with MAPLA treatment enhances the heterogeneous nucleation effect of the fibers leading to higher extent of cold crystallization during the test. The ratio between the loss and storage moduli is defined as the loss factor or tan(δ) [tan(δ) = E″/E′]. This property represents a balance between the elastic and viscous contribution in the composite. A lower magnitude of tan(δ) is expected for composites with a strong interface which will sustain higher stress and dissipate less energy [15]. The tan(δ) of the composites is presented in Fig. 8b. The addition of higher fiber contents decreased the magnitude of tan(δ) since the fibers restrict the movement of the polymer chains and change the matrix crystallinity [23]. However, the tan(δ) at 20 and 30% TAF exhibit further decreases as consequence of better compatibility. In particular, improved interfacial adhesion was observed at 20% of fiber content. Le Moigne et al. [12] also

reported lower tan(δ) with organosilane surface treatments because of the formation of a strong interface with reduced molecular mobility. They also suggested that interactions occurring at the interface tend to reduce the tan(δ) because of the formation of a layer of immobilized chains (steric hindrance), assuming that chemical and mechanical interlocking occurred at the interface.

Thermal Analysis

Figure 9 shows the DTG curves of the untreated and treated biocomposites. For the UFBC, the onset degradation temperature, defined as the temperature for 98% of the original weight ($T_{98\%}$), slightly decreased with fiber content. However, the trend is not clear since good dispersion was not achieved without surface treatment. Conversely, the DTG curves for TFBC clearly show a decreasing trend of the onset temperature with increasing fiber content. The introduction of fibers decreases the thermal stability of PLA due to the degradation of lignocellulosic materials occurring between 140 and 370 °C. The $T_{98\%}$ for neat PLA is 288 °C, while the addition of 10% agave decreases it to 254 °C. However, a slight increase (12 °C) of $T_{98\%}$ (from 254 to 266 °C) is observed for TFBC in comparison with UFBC at 10% agave fibers as a result of chemical bonding at the interface [15].

Water Absorption

Figure 10 presents the water absorption curves for UFBC and TFBC. In both cases, increasing the amount of fiber increases the water absorption of the biocomposite because of the high amount of hydroxyl groups on natural fibers [46]. However, in all cases, water absorption is much lower in TFBC, indicating that the polymer layer on the fibers' surface decreases their hydrophilicity because of the
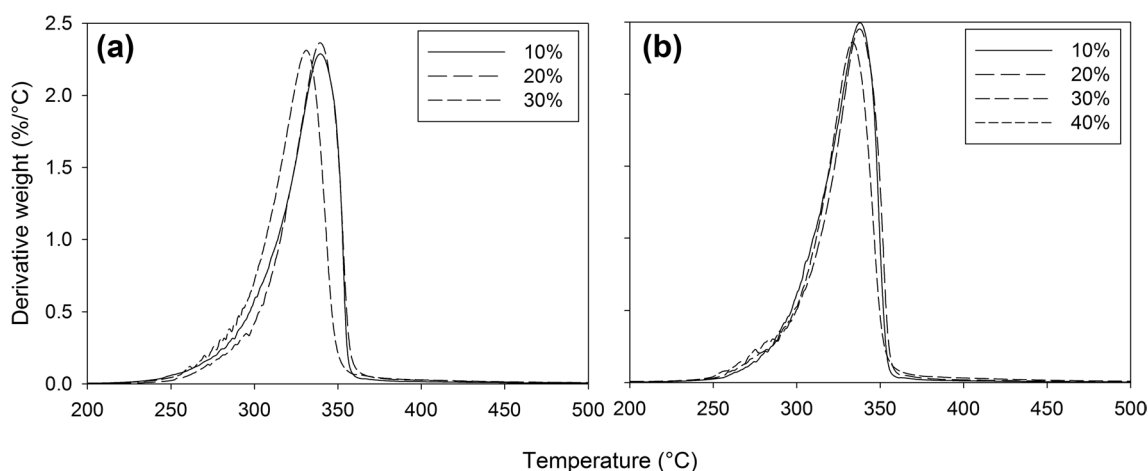

Fig. 9 DTG curves for: (a) untreated and (b) treated fiber composites at different agave contents
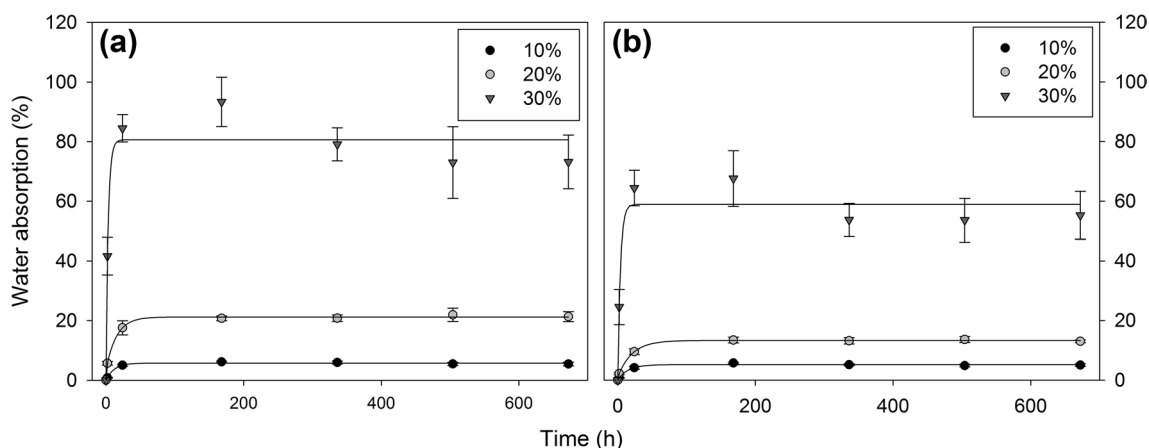
Fig. 10 Water absorption curves of: (**a**) UFBC and (**b**) TFBC at different agave contents

esterification reaction decreasing the number of available hydroxyl groups on fibers (see Fig. 1). Furthermore, the surface treatment promotes better fiber wetting improving their resistance to water uptake. Rajesh et al. [46] reported lower water absorption after alkali treatment, suggesting that the alkali reaction with the sisal fibers improved hydrophobicity. Moreover, Lv et al. [24] confirmed that when composites are compatibilized through MA, better compatibility restricts the diffusion of water molecules into the composites related to the coupling reaction at the fiber surface. Here, water absorption was decreased by up to 39% at 20% of fiber content. The biocomposites with 30% agave showed a decrease after 200 h. As reported in the "Morphology" section, with increasing fiber content, the porosity increases (more gaps in the composite). This provides better access to water molecules causing material disintegration. This also increases the sorption kinetics as fiber content increases. Finally, the diffusion coefficients calculated from the Langmuir absorption model are reported in Table 1. It is clear that the treatment modified the fibers' hydrophilicity leading to lower diffusion coefficients of the biocomposites and this effect is more noticeable at higher fiber contents. The diffusion coefficient was found to decrease by 22% (1.30×10^{-8}–1.01×10^{-8} m^2/s) at 30% agave. These values are in agreement with others reported in literature [47]. Arbelaiz et al. [48] also reported

that MAPP addition decreased the diffusion coefficient in flax fiber/polypropylene composites since fewer gaps were produced because of improved interfacial adhesion and the presence of more hydrophobic groups on the fibers' surface. The other Langmuir parameters are also listed in Table 1. It is important to notice that β represents the probability of free moisture molecules to become bound (mainly through hydrogen bonding with cellulose hydroxyls) and this value increases with fiber content. At 30% agave, β drastically increases for UFBC as a consequence of increased fiber contented and porosity. Nevertheless, for TFBC it does not increase to the same extent. In the case of α, as it represents the probability of bound molecules to become free, it decreases with fiber content. However, water desorption seems to not be related with treatment. Finally, the equilibrium moisture content decreases with fiber surface treatment.

Conclusions

In this study, grafting MAPLA onto the surface of agave fibers was evaluated as a strategy to improve interfacial adhesion and to increase fiber content in rotomolded PLA-agave fiber biocomposites and a complete physical, mechanical and thermal characterization was performed to evaluate the

Table 1 Calculated parameters of the Langmuir diffusion model (Eq. 2)

Sample	Fiber content (% wt.)	D (10^{10} m^2/s)	M_∞ (%)	α (-)	β (-)	L (mm)
UFBC	10	6.8	5.7	0.949	0.348	2.125
	20	13.9	21.0	0.837	5.262	3.124
	30	130.0	80.2	0.805	210,565	5.082
TFBC	10	6.7	5.1	0.959	0.270	2.350
	20	8.7	13.1	0.823	12.160	3.096
	30	101.0	58.3	0.815	33.497	4.964

effect of the surface treatment on the biocomposite properties. Firstly, FTIR measurements confirmed that the solution treatment successfully produced a MAPLA layer on the fibers' surface. In terms of morphology, MAPLA treatment led to biocomposites with better fiber distribution and lower void content, interfacial gap and fiber pull-out. Furthermore, density increased with the treatment, in particular at higher fiber content, resulting in lower porosity. In general, improved compatibility promoted good stress transfer and increased the mechanical properties. Tensile strength and modulus showed increases by up to 68% (from 25 to 41 MPa) and 32% (from 1.30 to 1.74 GPa) respectively. In the case of flexural properties, slight increases were obtained at 10% wt. of treated agave fiber with flexural strength going from 50 to 55 MPa and flexural modulus from 2.4 to 3.0 GPa. These results proved that coating agave fibers with MAPLA is a suitable strategy to increase the amount of fiber that could be incorporated to the rotomolded biocomposites while maintaining acceptable properties since the mechanical behavior was enhanced at a fiber content of 20% wt. However, it was observed in both tensile and flexural properties that fiber contents above 20% wt. produced important decreases in mechanical properties indicating that the coupling strategy under conditions tested in this study (e.g., MAPLA concentration, temperature and contact time) was suitable in composites with up to 20% wt. of fiber content. Grafting MAPLA at the fibers' surface also decreased their hydrophilicity and promoted better fiber wetting. Moreover, lower water absorption (equilibrium content) and diffusion coefficient was reported for the biocomposites. In this study, water absorption decreased by up to 39% at 20% wt. of fiber content. In the case of DMTA, the storage modulus was found to increase with fiber treatment for all fiber contents, indicating that the stress was better transferred from the matrix to the fibers thus increasing the overall stiffness. In contrast, the damping behavior decreased with fiber concentration and further decrease was produced because of better compatibility since a strong interface is able to sustain higher stress levels and dissipate less energy. Finally, the thermal stability was improved due to chemical bonding at the interface leading to a slight increase (12 °C) of the onset degradation temperature (from 254 to 266 °C). Based on the above mentioned results, PLA-agave fiber biocomposites produced by rotational molding with enhanced physical, mechanical and thermal properties were successfully obtained by carrying out the surface treatment of agave fibers with MAPLA, which proved to be a suitable strategy to increase fiber content by improving the compatibility in the system.

References

1. Kwon HJ, Sunthornvarabhas J, Park JW, Lee JH, Kim HJ, Piyachomkwan K, Sriroth K, Cho D (2014) Compos Part B 56:232
2. Tokiwa Y, Calabia BP (2006) Appl Microbiol Biotechnol 72:244
3. Baheti V, Militky J, Marsalkova M (2013) Polym Compos 34:2133
4. Awal A, Rana M, Sain M (2015) Mech Mater 80:87
5. Auras R, Harte B, Selke S (2004) Macromol Biosci 4:835
6. Pérez-Fonseca AA, Robledo-Ortíz JR, González-Núñez R, Rodrigue D (2016) J Appl Polym Sci 133:43750
7. Greco A, Maffezzoli A (2016) Polym Degrad Stab 132:213
8. Jiang L, Wolcott MP, Zhang J (2006) Biomacromolecules 7:199
9. Zhang M, Thomas N (2011) Adv Polym Technol 2:67
10. Hinchcliffe SA, Hess KM, Srubar WV (2016) Compos Part B 95:346
11. Harmaen AS, Khalina AK, Azowa I, Hassan MA, Tarmian A, Jawaid M (2015) Polym Compos 36:576
12. Le Moigne N, Longerey M, Taulemesse JM, Bénézet JC, Bergeret A (2014) Ind Crop Prod 52:481
13. Avella M, Martuscelli E, Raimo M (2000) J Mater Sci 35:523
14. Huda MS, Drzal LT, Mohanty AK, Misra M (2008) Compos Sci Tech 68:424
15. Yu T, Ren J, Li S, Yuan H, Li Y (2010) Compos Part A 41:499
16. Luo H, Zhang C, Xiong G, Wan Y (2016) Polym Compos 37:3499
17. Orue A, Jauregi A, Unsuain U, Labidi J, Eceiza A, Arbelaiz A (2016) Compos Part A 84:186
18. Cisneros-López EO, Pérez-Fonseca AA, Fuentes-Talavera FJ, Anzaldo J, González-Núñez R, Rodrigue D, Robledo-Ortíz JR (2016) Polym Eng Sci 56:856
19. Cisneros-López EO, González-López ME, Pérez-Fonseca AA, González Núñez R, Rodrigue D, Robledo-Ortíz JR (2017) Compos Interface 24:35
20. Gunning MA, Geever LM, Killion JA, Lyons JG, Higginbotham CL (2014) Polym Compos 35:1792
21. Yu T, Jiang N, Li Y (2014) Compos Part A 64:139
22. Arias A, Heuzey MC, Huneault MA (2013) Cellulose 20:439
23. Nyambo C, Mohanty AK, Misra M (2011) Macromol Mater Eng 296:710
24. Lv S, Gu J, Tan H, Zhang Y (2016) J Appl Polym Sci 133:43295
25. Jiang A, Xu X, Wu H (2016) Polym Compos 37:802
26. Greco A, Maffezzoli M (2015) Adv Polym Technol 34:21505
27. Lu T, Liu S, Jiang M, Xu X, Wang Y, Wang Z, Gou J, Hui D, Zhou Z (2014) Compos Part B 62:191
28. Brewer CE, Chuang VJ, Masiello CA, Gonnermann H, Gao X, Dugan B, Driver LE, Panzacchi P, Zygourakis K, Davies CA (2014) Biomass Bioenerg 66:176
29. Martynenko A (2014) Dry Technol 32:1319
30. Xu H, Zhou J, Dong Q, Tan Y (2017) Mater Des 124:108
31. Carter HG, Kibler KG (1978) J Compos Mater 12:118
32. Orozco VH, Brostow W, Chonkaew W, López BL (2009) Macromol Symp 277:69
33. Verdaguer A, Rodrigue D (2014) Effect of surface treatment on the mechanical properties of wood-plastics composites produced by dry-blending. In: 72th annual technical conference & exhibition, Society of Plastics Engineers, Las Vegas, NV, USA
34. Korotkova E, Pranovich A, Wärnå J, Salmi T, Murzin DY, Willför S (2015) Green Chem 17:5058
35. Melo JDD, Carvalho LFM, Medeiros AM, Souto CRO, Paskocimas CA (2012) Compos Part B 43:2827
36. Jandas PJ, Mohanty S, Nayak SK (2011) Polym Compos 32:1689

37. Csikós Á, Faludi G, Domján A, Renner K, Móczó J, Pukánszky B (2015) Eur Polym J 68:592
38. Raymond A, Rodrigue D (2014) Effect of surface treatment on the properties of wood-plastics composites produced by rotomolding. In: 72th annual technical conference & exhibition, Society of Plastics Engineers, Las Vegas, NV, USA
39. Mahfoudh A, Cloutier A, Rodrigue D (2013) Polym Compos 34:510
40. Kaynak C, Meyva Y (2014) Polym Adv Technol 25:1622
41. Teymoorzadeh H, Rodrigue D (2015) J Bio Mater Bio 9:1
42. Kaymakci A, Ayrılmis N, Gülec T (2013) Bioresources 8:592
43. Bax B, Müssig J (2008) Compos Sci Technol 68:1601
44. Bledzki AK, Jaszkiewicz A, Scherzer D (2009) Compos Part A 40:404
45. Ning N, Fu S, Zhang W, Chen F, Wang K, Deng H, Zhang Q, Fu Q (2012) Prog Polym Sci 37:1425
46. Rajesh G, Prasad AR, Gupta A (2015) J Reinf Plast Compos 34:951
47. Orue A, Eceiza A, Peña-Rodriguez C, Arbelaiz A (2016) Materials 9:400
48. Arbelaiz A, Fernandez B, Ramos JA, Regegi A, Llano-Ponte R, Mondragon I (2005) Compos Sci Technol 65:1582